

Numerical solution method for the dbar-equation in the plane

K. Knudsen ^{a,*}, J. Mueller ^b and S. Siltanen ^c

^a *Department of Mathematical Sciences, Aalborg University, Fredrik Bajers Vej 7G, DK-9220 Aalborg Ø, Denmark*

^b *Department of Mathematics, Colorado State University, Fort Collins, CO 80523, USA*

^c *Instrumentarium Corp., Finland, and Department of Mathematics, Gunma University, Tenjin-cho 1-5-1, 376-8515 Kiryu, Japan*

Abstract

A fast method for solving $\bar{\partial}$ -equations of the form $\bar{\partial}v = T\bar{v}$ is presented, where v and T are complex-valued functions of two real variables. The multigrid method of Vainikko [*Direct and inverse problems of mathematical physics*, Int. Soc. Anal. Appl. Comput., 5, Kluwer 2000] is adapted to the problem with a FFT implementation. Convergence with rate $\mathcal{O}(h)$ is proved for the method applied to equations of the form above. One-grid and two-grid versions of the method are implemented and their effectiveness is demonstrated on an application arising in electrical impedance tomography (EIT).

Key words: inverse scattering, dbar-equation, FFT, electrical impedance tomography, multigrid method

1 Introduction

In this paper we consider the numerical computation of the solution $v : \mathbb{R}^2 \rightarrow \mathbb{C}$ to the $\bar{\partial}$ -equation

$$\bar{\partial}v(k) = -T(k)\overline{v(k)} \quad (1.1)$$

* Corresponding author

Email addresses: kim@math.auc.dk (K. Knudsen), mueller@math.colostate.edu (J. Mueller), samuli.siltanen@iki.fi (S. Siltanen).

with the asymptotic condition $\lim_{|k| \rightarrow \infty} v(k) = 1$. Here the $\bar{\partial}$ -operator is defined by

$$\bar{\partial} = \bar{\partial}_k = \frac{\partial}{\partial \bar{k}} = \frac{1}{2} \left(\frac{\partial}{\partial k_1} + i \frac{\partial}{\partial k_2} \right) \quad (1.2)$$

and the multiplier $T : \mathbb{R}^2 \rightarrow \mathbb{C}$ is assumed to have compact support. In the sequel we identify $k \in \mathbb{R}^2$ with $k \in \mathbb{C}$ and use $k = (k_1, k_2)$ and $k = k_1 + ik_2$ interchangeably.

By convolving in (1.1) with the Green's function $1/\pi k$ for $\bar{\partial}$, it follows that the equation (1.1) together with the asymptotic condition is equivalent to the integral equation

$$v(k) = 1 - \frac{1}{\pi} \int_{\mathbb{R}^2} \frac{T(k')}{k - k'} \overline{v(k')} dk'_1 dk'_2, \quad k = k'_1 + ik'_2 \in \mathbb{C}, \quad (1.3)$$

or

$$v(k) = 1 - \frac{1}{\pi k} * (T(k) \overline{v(k)}) \quad (1.4)$$

where $*$ denotes convolution. We consider (1.4) as an equation in an appropriate function space on a bounded domain containing the support of T , and to solve this equation numerically we adapt the multigrid method introduced by Vainikko [37]. This method is a fast method based on FFT for solving integral equations with weakly singular kernels.

The equation (1.1) arises in connection with problems in inverse scattering and nonlinear evolution equations. In the context of inverse scattering, the idea behind the $\bar{\partial}$ -method is to apply the $\bar{\partial}$ -operator to an integral equation that governs the solution of the scattering problem and derive a $\bar{\partial}$ -equation that the solution satisfies. This method leads to linear integral equations for reconstructing the eigenfunctions and the potential and also provides necessary conditions which the scattering data must satisfy. The $\bar{\partial}$ -method was first used by Beals and Coifman [6] for the quantum inverse scattering problem in 1-D and was extended to 2-D problems in [2] in the context of the Kadomtsev-Petviashvili (KP) equation which has applications in water waves, stratified fluids and plasma physics. See also the references [7,8,18,28,31] for applications to multidimensional problems. More recently, the $\bar{\partial}$ -method has been used in inverse problems in medical imaging including in electrical impedance tomography (EIT) by Nachman [26,27] and Brown-Uhlmann [11] and in positron-emission tomography (PET) by R. Novikov [29,30]. Out of the numerous nonlinear evolution equations where equation (1.1) is useful, we single out the Novikov-Veselov equations introduced by Novikov and Veselov [40] and considered by Boiti et al. [10] and Tsai [36] and the Davey-Stewartson equations [15,1].

The numerical solution of equation (1.1) was considered by Siltanen, Mueller and Isaacson [34] for EIT in the numerical algorithm based on Nachman's

uniqueness proof for the 2-D inverse conductivity problem [26]. In [34,35,24,25] equation (1.1) was solved numerically by a 2-D adaptation of the method of product integrals [4]. The numerical solution of equation (1.1) has also been applied to EIT by Knudsen [20] in the numerical algorithm based on the Brown-Uhlmann uniqueness proof for the 2-D inverse conductivity problem [11]. A fast, direct algorithm for the Lippmann–Schwinger equation in two dimensions is found in [13].

We describe both one– and two–grid implementations of Vainikko’s method. Details of this method for the Lippmann–Schwinger equation can be found in [38,33]. This method has been implemented in [24] for the computation of Faddeev’s exponentially growing solutions [17] and in [19] for the numerical computation of the solution to a scattering problem. Furthermore, we will discuss the complexity and accuracy of the method and show that the complexity of the method is $\mathcal{O}(M^2 \log(M))$ for obtaining the solution with accuracy order $\mathcal{O}(h)$, $h = C/M$, on a plane grid of size M^2 .

This paper is organized as follows. In section 2 we give the details of the fast algorithm and in section 3 we describe the two–grid extension. Then in section 4 we analyze the accuracy and complexity of the method. Finally in section 5 we provide an example of the application of the method to electrical impedance tomography.

2 The fast algorithm

In this section we describe a fast algorithm for numerical solution of the integral equation (1.3). The method is based on the work of Vainikko [37].

We wish to consider the equation (1.3) in the space $C^{0,1}(\mathbb{R}^2)$, the space of Lipschitz continuous and bounded functions on \mathbb{R}^2 . A suitable assumption on the function T is then the following:

A1 *Properties of T .* We assume that T is compactly supported in an open set Ω and that $T \in C^{0,1}(\mathbb{R}^2)$.

With such T the equation (1.3) is uniquely solvable:

Lemma 2.1 *Assume T satisfies assumption A1. Then (1.3) has a unique solution $v \in C^{0,1}(\mathbb{R}^2)$ with the property that $v - 1 \in L^p(\mathbb{R}^2)$, $2 < p < \infty$.*

Proof. It is well known that when $T \in L^2(\mathbb{R}^2)$ is compactly supported then the integral equation (1.3) has a unique solution v which satisfies the condition $(v - 1) \in L^p(\mathbb{R}^2)$ for $2 < p < \infty$ (see for instance [22, Proposition 2.2] for a proof of this fact).

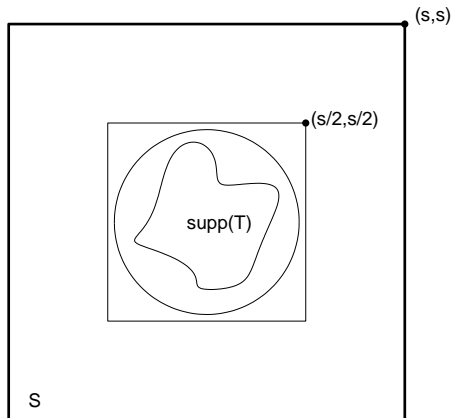


Fig. 1. The large square S determines the periodization of the $\bar{\partial}$ -equation. The circle and both of the squares are centered at the origin, and the radius of the circle is ρ .

Concerning the smoothness of v we note that $T\bar{v} \in L^p(\mathbb{R}^2)$, and hence $v - 1 = -(\pi k)^{-1} * (T\bar{v}) \in C^{0,\alpha}(\mathbb{R}^2)$ for any $\alpha < 1$, see [39, Thm. 1.21]. From this fact we deduce that $Tv \in C^{0,\alpha}(\mathbb{R}^2) \cap L^p(\mathbb{R}^2)$ and hence from [39, Thm. 1.34] we conclude that $v - 1 = -(\pi k)^{-1} * (Tv) \in C^{1,\alpha}(\mathbb{R}^2)$. The claim now follows from the continuous embedding $C^{1,\alpha}(\mathbb{R}^2) \subset C^{0,1}(\mathbb{R}^2)$. \square

The fast algorithm is based on the following crucial observations:

- If we know $v(k)$ for $k \in \text{supp}(T)$, we can compute v in the whole plane by $v = 1 - (\pi k)^{-1} * (T\bar{v})$.
- Let $\rho > 0$ be such that $\text{supp}(T) \subset B(0, \rho)$, where $B(0, \rho)$ is the open disc with radius ρ and center at the origin. If $k \in \text{supp}(T)$ then the integral in (1.4) does not involve the values of the convolution kernel $(\pi k')^{-1}$ for $|k'| \geq 2\rho$.

We will consider a periodic equation allowing fast solution and giving the solution to the full-plane equation. Choose $s > 2\rho$ and set $S := (-s, s)^2$; see Figure 1. Consider the following equation for functions that are $2s$ -periodic in k_1 and k_2 :

$$w(k) = f(k) - \int_{-s}^s \int_{-s}^s g(k - k') T(k') \overline{w(k')} dk'_1 dk'_2, \quad (2.1)$$

or more briefly

$$[I + g * (T \cdot \bar{\cdot})]w = f, \quad (2.2)$$

where $*$ denotes convolution on the torus and f satisfies the following:

A2 *Smoothness of f* . We assume that $f \in C^{0,1}(\mathbb{R}^2)$ is $2s$ -periodic in k_1, k_2 .

Clearly, $f \equiv 1$ satisfies A2. The $2s$ -periodic function g appearing in (2.1) and (2.2) is given by $g(k) = (\pi k)^{-1}$ for $k \in S$. (It is also possible to truncate g

sharply or smoothly at $|k| = 2\rho$). It is easily checked that

$$v|_{\text{supp}(T)} = w|_{\text{supp}(T)},$$

and that unique solvability of (1.3) is equivalent to that of (2.1) with $f \equiv 1$.

Next we discretize equation (2.2). Choose a positive integer m , denote $M = 2^m$, and set $h = 2s/M$. Note that the choice of M is taken mainly for simplicity; the algorithm would work just as well when M is a product of small primes. Define a grid $\mathcal{G}_m \subset \overline{S}$ by

$$\begin{aligned} \mathcal{G}_m &= \{jh \mid j \in \mathbb{Z}_m^2\}, \\ \mathbb{Z}_m^2 &= \{j = (j_1, j_2) \in \mathbb{Z}^2 \mid -2^{m-1} \leq j_l < 2^{m-1}, l = 1, 2\}. \end{aligned} \quad (2.3)$$

Note that the number of points in \mathcal{G}_m is M^2 . To each grid point $x \in \mathcal{G}_m$ we attach a *cell*, an open set that contains x . The cells are given by

$$B_{j,h} = \{(x_1, x_2) \in \mathbb{R}^2 \mid (j_l - \frac{1}{2})h < x_l < (j_l + \frac{1}{2})h, l = 1, 2\} \quad (2.4)$$

for $j \in \mathbb{Z}_m^2$.

Let $\varphi : \mathbb{R}^2 \rightarrow \mathbb{C}$ be a $2s$ -periodic function that is continuous, and define the grid approximation $\varphi_h : \mathbb{Z}_m^2 \rightarrow \mathbb{C}$ of φ by

$$\varphi_h(j) = \varphi(jh). \quad (2.5)$$

However, the Green's function $(\pi k)^{-1}$ is singular at $k = 0$, and (2.5) cannot be readily used. We set

$$g_h(j) = \begin{cases} g(jh), & \text{for } j \in \mathbb{Z}_m^2 \setminus 0, \\ 0, & \text{for } j = 0, \end{cases} \quad (2.6)$$

and since the singularity at $k = 0$ is integrable, the error caused by (2.6) becomes small when the discretization is refined.

We discretize the periodic convolution operator

$$(A\varphi)(k) = (g * \varphi)(k) = \int_{-s}^s \int_{-s}^s g(k - k')\varphi(k')dk'_1 dk'_2 \quad (2.7)$$

with the formula

$$A_h\varphi_h = \mathcal{F}^{-1}(\mathcal{F}g_h \cdot \mathcal{F}\varphi_h), \quad (2.8)$$

where \mathcal{F} is the discrete Fourier transform and \cdot denotes component-wise multiplication. The practical value of formula (2.8) is that application of the operator A_h can be implemented using the fast Fourier transform.

The discrete version of (2.2) is now

$$[I_h + A_h(T_h \cdot \cdot)]w_h = f_h, \quad (2.9)$$

where I_h denotes the identity matrix of size M^2 and $T_h \cdot \cdot$ denotes component-wise multiplication by the matrix $[T_h(j)]$. Solvability of this equation (for sufficiently large m) is a consequence of the solvability of (2.1). To avoid explicit representation of the inverse operator $[I_h + A_h(T_h \cdot \cdot)]^{-1}$ in the numerical solution of (2.9) we employ an iterative method, such as GMRES [32].

Note that since the operator $[I_h + A_h(T_h \cdot \cdot)]$ is real-linear but not complex linear, the real and imaginary parts of the complex solution vector w_h must be kept separate when using GMRES. An algorithm which avoids the use of the equivalent linear system of doubled size is found in [16].

3 Two-grid extension of the algorithm

We show how a two-grid method gives extra resolution with reasonable computational expense compared to solving (2.9) iteratively on one grid. We construct a two grid scheme with one fine grid and one coarse grid. We then solve (2.9) on the coarse grid and refine the solution on the fine grid.

Choose $0 < m^* < m$ and define the fine grid \mathcal{G}_m by (2.3) and its cells by (2.4). We next introduce the coarse grid \mathcal{G}_{m^*} and its *panels* B_{j^*,h^*}^* (we call the cells of the coarse grid panels). The following two requirements must be fulfilled [37, section 5.12]:

- R1 Every point of the coarse grid must belong to the fine grid: $\mathcal{G}_{m^*} \subset \mathcal{G}_m$.
- R2 Every cell $B_{j,h}$ of the fine grid must be contained in some panel B_{j^*,h^*}^* , and conversely, the closure of any panel must be the union of some collection of closures of fine grid cells.

Denote $M^* = 2^{m^*}$ and set $h^* = 2s/M^*$; then $0 < h < h^*$. Define the coarse grid \mathcal{G}_{m^*} equivalently to (2.3):

$$\mathcal{G}_{m^*} := \{j^*h^* \mid j^* \in \mathbb{Z}_{m^*}^2\}. \quad (3.1)$$

Requirement R1 clearly holds: the coarse grid is an equispaced collection of points in \mathcal{G}_m . The definition of panels must, however, be different from the definition of fine grid cells: the coarse grid points cannot be centerpoints of square cells without violating R2. We give the following definition as a compromise:

$$B_{j^*,h^*}^* := \text{int}\left(\bigcup_{j \in J_{j^*}} \overline{B_{j,h}}\right), \quad (3.2)$$

where int denotes topological interior and

$$J_{j^*} := \{j \in \mathbb{Z}_m^2 \mid j_l^* \leq j_l < j_l^* + 2^{m-m^*} h, \ l = 1, 2\}.$$

An illustration of the coarse and fine grids is found in figure 2. Definitions (2.5) and (2.6) apply for the coarse grid just by changing j to j^* and h to h^* .

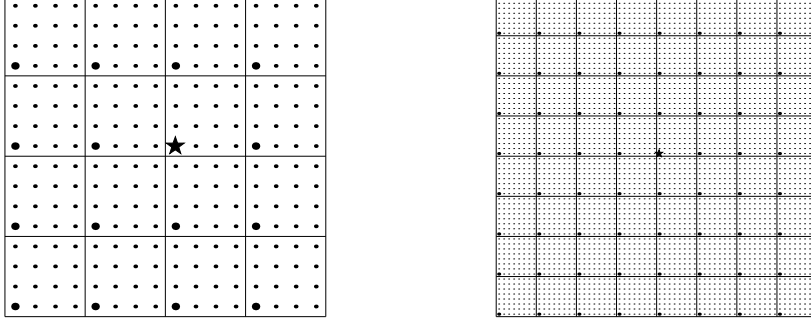


Fig. 2. Left: coarse and fine grid of the two-grid method corresponding to $m^* = 2$ and $m = 4$. Small dots denote the points of the fine grid and big dots denote the points of the coarse grid. Star denotes the origin (that belongs to both grids). Lines indicate boundaries of panels. Note that the coarse grid collocation points are regularly distributed but are not at the center of panels. Right: same as left plot but $m^* = 3$ and $m = 6$.

We require operators for transitions from one grid to the other. The operator p_{hh^*} taking functions $\mathbb{Z}_{m^*}^2 \rightarrow \mathbb{C}$ on the coarse grid to functions $\mathbb{Z}_m^2 \rightarrow \mathbb{C}$ on the fine grid is defined by piecewise constant interpolation:

$$(p_{hh^*} w_{h^*})(j) = w_{h^*}(j^*) \text{ for unique } j^* \in \mathbb{Z}_{m^*}^2 \text{ for which } B_{j,h} \subset B_{j^*,h^*}. \quad (3.3)$$

The fine-to-coarse operator p_{h^*h} is simply restriction:

$$(p_{h^*h} w_h)(j^*) = w_h(j) \text{ for unique } j \in \mathbb{Z}_m^2 \text{ for which } jh = j^*h^*. \quad (3.4)$$

The two-grid scheme is based on the observation that the solution w_h of (2.9) satisfies

$$w_h = f_{hh^*}'' - \mathcal{T}_{hh^*}'' w_h \quad (3.5)$$

where

$$f_{hh^*}'' = f_h - p_{hh^*}(I_{h^*} + A_{h^*}(T_{h^*} \cdot \cdot^{-}))^{-1} p_{h^*h} A_h(T_h \cdot \cdot^{-}) f_h,$$

and the operator \mathcal{T}_{h,h^*}'' is defined by

$$\mathcal{T}_{h,h^*}'' = [I_h - p_{hh^*}(I_{h^*} + A_{h^*}(T_{h^*} \cdot \cdot^{-}))^{-1} p_{h^*h}(I_h + A_h(T_h \cdot \cdot^{-}))] A_h(T_h \cdot \cdot^{-}). \quad (3.6)$$

The point is that when h^* is sufficiently small then the operator norm of \mathcal{T}_{h,h^*}'' is small (see (4.15) below), and hence $I + \mathcal{T}_{h,h^*}''$ can be inverted by a Neumann

series, and the solution to (3.5) can be computed by

$$w_h = (I_h + \mathcal{T}_{h,h^*}'')^{-1} f_{h,h^*}'' = \sum_{n=0}^{\infty} (-\mathcal{T}_{h,h^*}'')^n f_{h,h^*}''.$$

By using again (4.15) it is easy to verify that the Neumann series can be approximated by using the recursive formula

$$w_h^N = -\mathcal{T}_{h,h^*}'' w_h^{N-1} + f_{h,h^*}''$$

with any given initial choice for w_h^0 . For our purpose the natural choice for w_h^0 is the coarse grid solution. This gives the following two-grid scheme for computing an approximate solution to (2.9):

$$\begin{aligned} w_h^0 &= p_{hh^*} w_{h^*}, \\ \text{For } n = 0 : (N - 1) & \\ r_h^n &= w_h^n + A_h(T_h \cdot \bar{w}_h^n) - f_h \\ w_h^{n+1} &= w_h^n - r_h^n - p_{hh^*} (I_{h^*} + A_{h^*}(T_{h^*} \cdot \bar{\cdot}))^{-1} p_{h^*h} A_h(T_h \cdot \bar{r}_h^n) \end{aligned} \tag{3.7}$$

Note that m^* has to be large enough for the inverse of the coarse grid operator $(I_{h^*} + A_{h^*}(T_{h^*} \cdot \bar{\cdot}))$ to exist. This operator is then inverted using the one-grid scheme described in section 2.

When we want to apply the two-grid method for solving (2.9) on a grid of size given by the parameter m , the size of the coarse grid given by the parameter m^* and the iteration number N has to be chosen. These choices are related to the accuracy of the method and will be discussed in section 4.

4 Accuracy and complexity of the method

The one-grid method described in section 2 is inspired by method (5.13) in [37], but since our assumptions are slightly different, the convergence rates in [37, Theorem 5.1] are not immediate. However, the expected convergence rates follow from a proof analogous to that of [37, Theorem 5.1]. We will outline the main steps below.

The theory of discrete convergence is used in [37] to analyze the convergence of the discretization method. We also adopt this language for the proofs. The following definitions are taken from [37].

Definition 4.1 *Let E be a Banach space and let E_h be a family of Banach spaces parameterized by $h \geq 0$ (all spaces real or all complex). Let*

$p_h \in \mathcal{B}(E, E_h)$ be the so-called connection operators satisfying

$$\|p_h u\|_{E_h} \rightarrow \|u\|_E.$$

A family $\{u_h\}_{0 < h < H}$ of elements $u_h \in E_h$ is called discretely convergent to an element $u \in E$ if $\|u_h - p_h u\|_{E_h} \rightarrow 0$ as $h \rightarrow 0$.

Definition 4.2 A family $\{u_h\}$ of elements $u_h \in E_h$ is called discretely compact if any sequence $\{u_{h_n}\}$ formed by the elements of the family with $h_n \rightarrow 0$ contains a discretely convergent subsequence.

Definition 4.3 A family of linear bounded operators $T_h \in L(E_h, E_h)$ is called discretely convergent to $T \in L(E, E)$ if the following implication holds: discrete convergence of a family of elements $\{u_h\} \in E_h$ to an element $u \in E$ implies discrete convergence of $T_h u$ to Tu .

Definition 4.4 The bounded linear operator T_h converges to T discretely compactly if the implication in definition 4.3 holds and

$$\limsup_{h \rightarrow 0} \|u_h\|_{E_h} < \infty \quad \text{implies} \quad \{T_h u_h\} \quad \text{is discretely compact.} \quad (4.1)$$

We extend definitions 4.3 and 4.4 to include conjugate linear operators. Note that Lemmas 4.1, 4.2 and Theorem 4.1 of [37] hold for conjugate linear operators as well.

For our purpose we let $E = C(S)$, the set of continuous functions on the set S equipped with the supremum norm, and let $E_h = \mathcal{M}_{2^m \times 2^m}$ be the space of $2^m \times 2^m$ matrices equipped with the supremum norm. Further, we define the connection operators $p_h \in \mathcal{B}(E, E_h)$ by $(p_h \phi)(j) = \phi(jh)$, $j \in \mathbb{Z}_m^2$.

Theorem 4.1 Let conditions A1 and A2 hold for equation (2.2). Then there exists $m_0 > 0$ such that for $m > m_0$ the system (2.9) has a unique solution w_h with

$$\max_{j \in \mathbb{Z}_m^2} |w_h(j) - w(jh)| \leq Ch, \quad (4.2)$$

where $h = 2s/2^m$ and w is the unique solution to (2.2).

Proof. Define the operators $\mathcal{T} \in \mathcal{B}(E)$, $\mathcal{T}_h, \mathcal{T}_h'' \in \mathcal{B}(E_h)$ by

$$\begin{aligned} \mathcal{T}u(k) &= \frac{1}{\pi} \int_S \frac{T(k')}{k - k'} \overline{u(k')} dk'_1 dk'_2, \quad k \in S \\ \mathcal{T}_h u_h(j) &= \frac{1}{\pi} \sum_{l \in \mathbb{Z}_m^2} \int_{B_{l,h}} \frac{T(k')}{jh - k'} dk'_1 dk'_2 \overline{u_h(l)}, \\ \mathcal{T}_h'' u_h(j) &= h^2 \sum_{l \in \mathbb{Z}_m^2} g_h(j - l) T_h(l) \overline{u_h(l)}. \end{aligned}$$

Note that these operators are compact. The proof is divided into three steps:

- (1) Show the existence of $h_0 > 0$ such that for $0 < h < h_0$ the system (2.9) has a unique solution w_h with

$$\max_{j \in \mathbb{Z}_m^2} |w_h(j) - w(jh)| \leq C \|\mathcal{T}_h'' p_h w - p_h \mathcal{T} w\|_{E_h}. \quad (4.3)$$

- (2) Show that

$$\|\mathcal{T}_h p_h w - p_h \mathcal{T} w\|_{E_h} \leq Ch \quad (4.4)$$

for the solution $w \in E$ to (2.2).

- (3) Show that

$$\|\mathcal{T}_h - \mathcal{T}_h''\|_{\mathcal{B}(E_h)} \leq Ch. \quad (4.5)$$

It is clear that (4.2) follows from (4.3) – (4.5) by the triangle inequality.

Claim (1) follows from [37, Theorem 4.1], since $\mathcal{T}_h \rightarrow \mathcal{T}$ discretely compactly. For a complete proof of this fact we refer to the proof of [37, Lemma 5.2], which is easily adapted to our setting.

To prove (4.4) we use the fact that the solution w to (2.2) is Lipschitz continuous in S . Hence it follows that

$$\begin{aligned} \|\mathcal{T}_h p_h w - p_h \mathcal{T} w\|_{E_h} &= \max_{j \in \mathbb{Z}_m^2} \left| \sum_{l \in \mathbb{Z}_m^2} \int_{B_{l,h}} \frac{T(k')}{jh - k'} \overline{(p_h w(l) - w(k'))} dk'_1 dk'_2 \right| \\ &\leq \max_{k \in S} |T(k)| \int_S \frac{1}{|k - k'|} dk'_1 dk'_2 \max_{\substack{l \in \mathbb{Z}_m^2 \\ z_1, z_2 \in B_{l,h}}} |w(z_1) - w(z_2)| \\ &\leq C \max_{\substack{l \in \mathbb{Z}_m^2 \\ z_1, z_2 \in B_{l,h}}} |z_1 - z_2| \\ &\leq Ch. \end{aligned}$$

Concerning (4.5) note that

$$\|\mathcal{T}_h - \mathcal{T}_h''\|_{\mathcal{B}(E_h)} = \max_{j \in \mathbb{Z}_m^2} \sum_{l \in \mathbb{Z}_m^2} |\mathcal{T}_{jl,h} - \mathcal{T}_{jl,h}''|,$$

where for $j, l \in \mathbb{Z}_m^2$

$$\begin{aligned} \mathcal{T}_{jl,h} &= \int_{B_{l,h}} \frac{T(k')}{jh - k'} dk'_1 dk'_2, \\ \mathcal{T}_{jl,h}'' &= \begin{cases} h^2 \frac{T_h(l)}{jh - lh}, & l \neq j, \\ 0, & l = j. \end{cases} \end{aligned}$$

By using the Lipschitz continuity of T it can then be proved that

$$\begin{aligned} \sum_{l \neq j} |\mathcal{T}_{jl,h} - \mathcal{T}_{jl,h}''| &= \sum_{l \neq j} \left| \int_{B_{l,h}} \left(\frac{T(k')}{jh - k'} - \frac{T(lh)}{jh - lh} \right) dk'_1 dk'_2 \right| \\ &\leq Ch. \end{aligned}$$

Moreover,

$$|\mathcal{T}_{jj,h}| = \left| \int_{B_{j,h}} \frac{T(k')}{jh - k'} dk'_1 dk'_2 \right| \leq \max_{k \in B_{j,h}} |T(k)| \int_{|k'| < \sqrt{2}h} \frac{1}{|k'|} dk'_1 dk'_2 \leq Ch.$$

Hence

$$\begin{aligned} \|\mathcal{T}_h - \mathcal{T}_h''\|_{\mathcal{B}(E_h)} &= \max_{j \in \mathbb{Z}_m^2} (|\mathcal{T}_{jj,h}| + \sum_{l \neq j} |\mathcal{T}_{jl,h} - \mathcal{T}_{jl,h}''|) \\ &\leq Ch. \end{aligned}$$

□

Concerning the complexity of the one-grid method we note that with an FFT implementation one application of the discrete convolution operator (2.8) is done in $\mathcal{O}(M^2 \log M)$ arithmetical operations. Hence to solve (2.9) using an iterative solver with a fixed upper bound on the numbers of iterations also requires $\mathcal{O}(M^2 \log M)$ arithmetical operations.

Recall the definition of the operator \mathcal{T}_{h,h^*}'' from (3.6) and note that

$$\mathcal{T}_{h,h^*}'' = (I_h - p_{hh^*} p_{h^*h}) \mathcal{T}_h'' + p_{hh^*} (I_{h^*} + \mathcal{T}_{h^*})^{-1} (p_{h^*h} \mathcal{T}_h'' - \mathcal{T}_{h^*}'' p_{h^*h}) \mathcal{T}_h''.$$

Define \mathcal{T}_{h,h^*} by

$$\begin{aligned} \mathcal{T}_{h,h^*} &= [I_h - p_{hh^*} (I_{h^*} + \mathcal{T}_{h^*})^{-1} p_{h^*h} (I_h + \mathcal{T}_h)] \mathcal{T}_h \\ &= (I_h - p_{hh^*} p_{h^*h}) \mathcal{T}_h + p_{hh^*} (I_{h^*} + \mathcal{T}_{h^*})^{-1} (p_{h^*h} \mathcal{T}_h - \mathcal{T}_{h^*} p_{h^*h}) \mathcal{T}_h \end{aligned} \quad (4.6)$$

We first prove a lemma needed to establish the convergence rate of the two-grid method.

Lemma 4.1 *For h^* sufficiently small and $0 < h < h^*$ we have*

$$\|\mathcal{T}_{h,h^*}\|_{\mathcal{B}(E_h, E_{h^*})} \leq Ch^* \log h^*.$$

Proof. We want to prove that

$$\|(I_h - p_{hh^*} p_{h^*h}) \mathcal{T}_h\|_{\mathcal{B}(E_h)} \leq Ch^* \log h^*, \quad (4.7)$$

$$\|(p_{h^*h} \mathcal{T}_h - \mathcal{T}_{h^*} p_{h^*h}) \mathcal{T}_h\|_{\mathcal{B}(E_h)} \leq Ch^* \log h^*. \quad (4.8)$$

Then the conclusion follows from (4.6) and the fact that for h^* sufficiently small, the operator $I_{h^*} + \mathcal{T}_{h^*}$ is invertible with uniformly bounded inverse (see [37, Lemma 4.2]).

For $w_h \in E_h$, define the piecewise constant function $\hat{w}_h \in E$ by

$$\hat{w}_h(k) = \sum_{j \in \mathbb{Z}_m^2} w_h(j) \xi_{j,h}(k), \quad (4.9)$$

where

$$\xi_{j,h}(k) = \begin{cases} 1, & \text{if } k \in B_{j,h}, \\ 0, & \text{otherwise.} \end{cases} \quad (4.10)$$

Then $\|\hat{w}_h\|_E = \|w_h\|_{E_h}$ and

$$\begin{aligned} \mathcal{T}\hat{w}_h(jh) &= \frac{1}{\pi} \int_S \frac{T(k')}{jh - k'} \overline{\hat{w}_h(k')} dk'_1 dk'_2 \\ &= \frac{1}{\pi} \sum_{l \in \mathbb{Z}_m^2} \int_{B_{l,h}} \frac{T(k')}{jh - k'} dk'_1 dk'_2 \overline{w_h(l)} \\ &= \mathcal{T}_h w_h(j). \end{aligned}$$

From [39, Theorem 1.22] it is known that

$$|\mathcal{T}u(x) - \mathcal{T}u(y)| \leq C \|u\|_E |x - y| \log(|x - y|).$$

In particular we have

$$|\mathcal{T}\hat{w}_h(lh) - \mathcal{T}\hat{w}_h(jh)| \leq C \|\hat{w}_h\|_E |lh - jh| \log(|lh - jh|), \quad (4.11)$$

which implies

$$|\mathcal{T}_h w_h(l) - \mathcal{T}_h w_h(j)| \leq C \|w_h\|_{E_h} |lh - jh| \log(|lh - jh|). \quad (4.12)$$

By (3.3) and (3.4) we see that

$$\begin{aligned} |(I_h - p_{hh^*} p_{h^*h}) \mathcal{T}_h w_h(j)| &= |\mathcal{T}_h w_h(j) - p_{hh^*} p_{h^*h} \mathcal{T}_h w_h(j)| \\ &= |\mathcal{T}_h w_h(j) - \mathcal{T}_h w_h(j^*)|, \end{aligned}$$

where j^* is the unique $j^* \in \mathbb{Z}_{m^*}^2$ such that $B_{j,h} \subset B_{j^*,h^*}$. Then by (4.12)

$$|(I_h - p_{hh^*} p_{h^*h}) \mathcal{T}_h w_h(j)| \leq C \|w_h\|_{E_h} h^* \log(h^*),$$

since j and j^* are in the same panel. This gives (4.7).

Now let v_h denote $\mathcal{T}_h w_h$. Then

$$\begin{aligned}
((p_{h^*h}\mathcal{T}_h - \mathcal{T}_{h^*}p_{h^*h})v_h)(j^*) &= \mathcal{T}_h v_h(j^*) - \mathcal{T}_{h^*}p_{h^*h}v_h(j^*) \\
&= \frac{1}{\pi} \sum_{l \in \mathbb{Z}_m^2} \int_{B_{l,h}} \frac{T(k')}{j^*h - k'} dk'_1 dk'_2 v_h(l) \\
&\quad - \frac{1}{\pi} \sum_{l^* \in \mathbb{Z}_{m^*}^2} \int_{B_{l^*,h^*}} \frac{T(k')}{j^*h^* - k'} dk'_1 dk'_2 v_h(l^*) \\
&= \frac{1}{\pi} \sum_{l \in \mathbb{Z}_m^2} \int_{B_{l,h}} \frac{T(k')}{j^*h - k'} dk'_1 dk'_2 (v_h(l) - v_h(l^*))
\end{aligned}$$

where l^* is defined by (3.4). Since l and l^* are in the same panel we conclude that

$$|((p_{h^*h}\mathcal{T}_h - \mathcal{T}_{h^*}p_{h^*h})w_h)(j^*)| \leq \left(\sup_{k \in S} \int_S \left| \frac{T(k')}{k - k'} \right| dk'_1 dk'_2 \right) C \|w_h\|_{E_h} h^* \log(h^*),$$

which proves (4.8). \square

The following theorem gives the convergence rate of the two-grid method.

Theorem 4.2 *Let conditions A1 and A2 hold for equation (2.2). Then for sufficiently small $h^* > 0$ and $0 < h < h^*$, the function w_h^N in (3.7) satisfies*

$$\max_{j \in \mathbb{Z}_m^2} |w_h^N(j) - w_h(j)| \leq \max_{j \in \mathbb{Z}_m^2} |w_h^0(j) - w_h(j)| (Ch^* \log(h^*))^N, \quad (4.13)$$

where $N = 0, 1, 2, \dots$, and w_h is the unique solution to the discrete equation (2.9).

Proof. It follows as a consequence of (4.5) that

$$\|\mathcal{T}_{h,h^*}'' - \mathcal{T}_{h,h^*}\|_{\mathcal{B}(E_h)} \leq Ch^*. \quad (4.14)$$

Thus, (4.14) and Lemma 4.1 imply that

$$\|\mathcal{T}_{h,h^*}''\|_{\mathcal{B}(E_h)} \leq \|\mathcal{T}_{h,h^*}'' - \mathcal{T}_{h,h^*}\|_{\mathcal{B}(E_h)} + \|\mathcal{T}_{h,h^*}\|_{\mathcal{B}(E_h)} \leq Ch^* \log(h^*). \quad (4.15)$$

If $Ch^* \log(h^*) < 1$, then $\|\mathcal{T}_{h,h^*}''\| < 1$ and (3.5) is uniquely solvable. Thus, the iteration scheme (3.7) converges with rate of convergence

$$\|w_h^N - w_h\|_{E_h} \leq \|w_h^0 - w_h\|_{E_h} (Ch^* \log(h^*))^N, \quad N = 0, 1, 2, \dots$$

where C is independent of h and h^* . This proves the theorem. \square

Since the solution w_h to the discrete equation (2.9) converges by Theorem 4.1 to the solution w to the continuous equation (2.1) with rate $\mathcal{O}(h)$, and the

approximate solution w_h^N to (2.9) computed by the two-grid method converges to w_h with the rate given in Theorem 4.2, we can by choosing the parameters m^* and N ensure that also w_h^N converges to w with rate $\mathcal{O}(h)$. This is achieved when

$$\max_{j \in \mathbb{Z}_m^2} |w_h^0(j) - w_h(j)| (Ch^* \log(h^*))^N \leq Ch.$$

The choice of the initial guess in (3.7) gives by Theorem 4.1

$$\begin{aligned} \max_{j \in \mathbb{Z}_m^2} |w_h^0(j) - w_h(j)| &= \max_{j \in \mathbb{Z}_m^2} |p_{hh^*} w_{h^*}(j) - w_h(j)| \\ &\leq Ch^*, \end{aligned}$$

and hence we consider the inequality

$$h^{*N+1} \log(h^*)^N \leq Ch$$

for N and h^* . A reasonable choice for h^* is $h^* \sim h^{1/3}$, which implies that the desired accuracy will be reached asymptotically in $N = 3$ steps. Note that the choice $h^* \sim h^{1/3}$ implies that m^* should be chosen as

$$m^* = \left\lceil \frac{m-1}{3} \right\rceil + 1.$$

The complexity of the two-grid method is also $\mathcal{O}(M^2 \log(M))$, since the algorithm (3.7) involves the application of the discrete convolution operator (2.8) on the fine grid.

5 Application to the inverse conductivity problem

The inverse conductivity problem is the mathematical problem behind a recent method for medical imaging called Electrical Impedance Tomography (EIT). The problem is to recover a bounded and strictly positive conductivity γ in a body Ω from static electric measurements on the boundary of the body. See, for example, [14] for further information about EIT. We consider here the two-dimensional problem, i.e. $\Omega \subset \mathbb{R}^2$. If we apply a voltage potential $f \in H^{1/2}(\partial\Omega)$ on the boundary of Ω , a voltage distribution $u \in H^1(\Omega)$ is induced in Ω described uniquely as the solution to the conductivity equation

$$\nabla \cdot \gamma \nabla u = 0 \text{ in } \Omega, \quad u = f \text{ on } \partial\Omega. \quad (5.1)$$

The voltage potential in Ω gives rise to a current flux through the boundary given by

$$\gamma \frac{\partial u}{\partial \nu} \Big|_{\partial \Omega},$$

which can be measured at the boundary. All possible boundary measurements are encoded in the map

$$\Lambda_\gamma : f \mapsto \gamma \frac{\partial u}{\partial \nu} \Big|_{\partial \Omega},$$

the so-called Dirichlet-to-Neumann map or voltage-to-current map that maps any voltage distribution on the boundary to the resulting current flux.

The inverse conductivity problem as considered by Calderón [12] consists of two questions. First, does the Dirichlet-to-Neumann map Λ_γ determine the conductivity γ uniquely, and then if so, how can the conductivity be reconstructed?

For sufficiently regular conductivities having essentially two derivatives Nachman [26] gave a uniqueness proof and a reconstruction algorithm, and for less regular conductivities with only one derivative Brown-Uhlmann [11] generalized the uniqueness result. Both methods are based on solving $\bar{\partial}$ -equations of the type (1.1). In this section we will outline a reconstruction method based on the latter approach and show how the implementations described above can be used in this context.

Let u be a solution to the conductivity equation (5.1) and identify $(z_1, z_2) \in \Omega$ with the complex number $z = z_1 + iz_2$. Then $(v, w) = \gamma^{1/2}(\partial_z u, \bar{\partial}_z u)$ solves the system

$$\begin{aligned} \bar{\partial}_z v &= qw, \\ \partial_z w &= \bar{q}v, \end{aligned} \tag{5.2}$$

where

$$q = -\gamma^{-1/2} \partial_z \gamma^{1/2}. \tag{5.3}$$

If we assume that $\gamma = 1$ near the boundary of Ω then q can be extended smoothly to \mathbb{R}^2 by setting $q = 0$ in $\mathbb{R}^2 \setminus \Omega$. The idea in the $\bar{\partial}$ -method of inverse scattering theory is then to look for a special exponentially growing solution $\Psi(z, k) = (\Psi_1, \Psi_2)(z, k)$ in \mathbb{R}^2 to the system (5.2) with

$$\Psi(z, k) = m(z, k) e^{izk}, \quad \lim_{|z| \rightarrow \infty} m(z, k) = \lim_{|z| \rightarrow \infty} (m_1, m_2) = (1, 0). \tag{5.4}$$

To construct m let $e(z, k) = \exp(i(zk + \overline{zk})) = \exp(i2\text{Re}(zk))$ and define

$$m_{\pm}(z, k) = m_1(z, k) \pm \overline{m_2(z, k)}e(z, -k). \quad (5.5)$$

This function satisfies by (5.2) and (5.4) the $\bar{\partial}$ -equation

$$\bar{\partial}_z m_{\pm}(z, k) = \pm q(z)e(z, -k)\overline{m_{\pm}(z, k)}, \quad \lim_{|z| \rightarrow \infty} m_{\pm}(z, k) = 1, \quad (5.6)$$

from which m_{\pm} can be recovered uniquely both theoretically and numerically. This also gives $m(z, k)$ by (5.5).

Associated with q is then the function

$$\mathcal{S}(k) = -\frac{i}{\pi} \int_{\Omega} e(z, k)\bar{q}(z)m_1(z, k)dz_1dz_2, \quad (5.7)$$

the so-called non-physical scattering transform of the potential q .

The usefulness of introducing the scattering transform in the solution of the inverse problem is two-fold. First, the scattering transform can be computed from boundary data [20,22], and second, the conductivity can be computed from \mathcal{S} . This gives a reconstruction procedure consisting of the two steps

$$\Lambda_{\gamma} \xrightarrow{1} \mathcal{S} \xrightarrow{2} \gamma.$$

Note that the stability analysis in [23,5] shows that the EIT problems is ill-posed and that the ill-posedness comes from the first step. The second step is actually well-posed. Here we will only consider the numerical implementation of the second step. See references [20,21,34,35,24] for complete implementations.

To compute γ from \mathcal{S} consider the $\bar{\partial}$ -equation in the parametric variable k ,

$$\bar{\partial}_k \tilde{m}^+(z, k) = \overline{\mathcal{S}(-k)}e(z, -k)\overline{\tilde{m}^+(z, k)}, \quad \lim_{|k| \rightarrow \infty} \tilde{m}^+(z, k) = 1. \quad (5.8)$$

This equation has the unique solution $\tilde{m}^+(z, k)$, which is highly related to $m(z, k)$ (see [20,22]). Moreover, from this solution we can compute

$$\gamma(z) = (\text{Re}(\tilde{m}^+(z, 0)))^2. \quad (5.9)$$

Hence by knowing \mathcal{S} , we can solve (5.8) and then obtain the γ from (5.9).

In the next subsections we will use the implementations described in section 2 and 3 to compute the scattering transform for a particular potential and reconstruct the conductivity from the scattering transform. First we will by solving (5.6) and using (5.7) compute the scattering transform of a particular potential defined from a conductivity by (5.3). Then we consider the inverse

problem and compute the conductivity from the scattering transform by solving (5.8) and using (5.9).

5.1 Test example

Our test example is a numerical chest phantom consisting of a heart and two lungs, where in one lung there is an abnormality. To simulate a cross-section of the chest during expiration, the conductivity of the phantom lungs was taken to be 1 mS/cm, the conductivity of the phantom heart was taken to be the approximate longitudinal conductivity of heart muscle, 6 mS/cm, and the background conductivity was chosen to be 3 mS/cm. The conductivity of the abnormality was taken to be 4 mS/cm to simulate a tumor. These conductivities were then scaled by dividing by 3 mS/cm so that the background conductivity is 1, the conductivity of the phantom heart is 2, the conductivity of the phantom lungs is .33, and the conductivity of the phantom tumor is 1.33. The phantom was then mollified so that the resulting conductivity is a smooth function on the unit circle; see the top row of Figure 3. For this conductivity we have computed the corresponding potential q by (5.3) using numerical differentiation.

We now compute the scattering transform $\mathcal{S}(k)$ on a 60×60 uniform k -mesh in the square $[-20, 20]^2$. First we solve the equation (5.6) for each k in the grid. Since the potential q is supported inside $[-1, 1]^2$ the equivalent periodic integral equation is

$$m_{\pm}(z, k) = 1 \pm \int_{-2}^2 \int_{-2}^2 \frac{q(z')e(z', k)}{z - z'} \overline{m_{\pm}(z', k)} dz_1 dz_2, \quad (5.10)$$

which can be solved numerically by the one- and two-grid implementations described in section 2 and 3. In the one-grid implementation we have chosen the grid-size $m = 7$, and in the two-grid implementation we have chosen $m^* = 3$, $m = 7$ and $N = 3$. Next, to compute \mathcal{S} we use the known function $e(z, k)\overline{q(z)}$ and the computed function $m_1(z, k) = m_+(z, k) + m_-(z, k)$ to evaluate the integral (5.7) by the trapezoid rule. Since (5.6) was solved both using the one- and two-grid implementations, we get two discrete approximations $\mathcal{S}_1, \mathcal{S}_2$ of \mathcal{S} . The relative l^∞ -difference of the two functions is approximately 1%.

Having computed the scattering transform we now consider the second step in the reconstruction algorithm for the inverse conductivity problem, the computation of γ from \mathcal{S} . First, we want to solve (5.8) for $\tilde{m}^+(z, k)$. Note that since \mathcal{S} is not compactly supported, the equation (5.8) is not readily in the form (1.1). Hence \mathcal{S} has to be truncated before the numerical implementations can be used and this cut-off will introduce a systematic error. However, since \mathcal{S} is a rapidly decaying function, the error can be neglected. In our computations

we have chosen to cut-off the scattering transform at $|k| = 20$, which reflects the support of the pre-computed approximations \mathcal{S}_1 and \mathcal{S}_2 . To compute the solution to (5.8) we therefore consider the periodic integral equation

$$\tilde{m}^+(z, k) = 1 + \int_{-40}^{40} \int_{-40}^{40} \frac{\overline{\mathcal{S}(-k')}e(z, -k')}{k - k'} \overline{\tilde{m}^+(z, k)} dk'_1 dk'_2,$$

which is solved using the one- and the two-grid implementations. In the one-grid method we choose the parameter $m = 7$ and use the approximation \mathcal{S}_1 , and in the two-grid method we choose $m = 7$, $m^* = 3$, $N = 3$, and use the approximation \mathcal{S}_2 . In both cases the conductivity is computed on a uniform 60×60 z -mesh in the square $[-1, 1]^2$. Next, to compute the conductivity we use (5.9), i.e. we evaluate the computed solutions to (5.8) at $k = 0$. This gives two reconstructions based on the one- and two-grid methods. The reconstructions are displayed in Figure 3. The relative l^∞ -difference of the two reconstructions is 3%, and the relative l^∞ -error in either of the reconstructions when compared to the true conductivity is approximately 6%.

We now compare the speed and the memory usage of the one-grid and two-grid method. For different values of the discretization level (given by the number m , where the size of each cell is h^2 for $h = 2^{-m}$) we have measured the speed and the memory requirements for computing $m_+(z, k)$ for fixed $k = 1$. For the two-grid method the number of iterations have been chosen according to the analysis in section 4 as $N = 3$. Table 5.1 contains the results for both methods.

m	m^*	Memory (in megabytes)		Speed (in seconds)	
		One-grid	Two-grid	One-grid	Two-grid
6	3	106	104	1	1
7	3	120	113	3	2
8	4	173	148	18	8
9	4	386	286	110	43
10	5	1252	836	450	176

Table 1

Speed and memory usage for computing the function $m_+(z, 1)$ by the one-grid and two-grid methods, respectively. The quantity m^* applies only to the two-grid computation.

It is clear that the two-grid is superior both concerning memory usage and speed.

Note that for both methods the speed decreases by approximately a factor 4, when going from a grid of size 2^m to a grid of size 2^{m+1} . This is expected since

the the complexity is $\mathcal{O}(M^2 \log(M)) = \mathcal{O}(m2^{2m})$ for $M = 2^m$.

Next we consider the accuracy of the one-grid method. Since the true solution $m_+(z, k)$ is not known explicitly, we have taken the most accurate approximation as the true solution and compared it to the other approximations. In this test we have again taken the parameter $k = 1$. Let $(m_+)_h$ denote the solution to the discrete version of (5.10) at discretization level $h = 2^{-m}$ and define the error

$$\mathcal{E}_m = \|(m_+)_h - p_{hh'}(m_+)_{h'}\|_{E_h},$$

where h' corresponds to the choice $m = 10$. As before $p_{hh'}$ denotes the transition operator from the fine grid to the coarse grid, and E_h is a space of matrices equipped with the sup-norm. Table 5.1 shows the results of the convergence analysis.

m	Error \mathcal{E}_m	Ratio $\mathcal{E}_m/\mathcal{E}_{m+1}$
3	0.5274	2.4
4	0.2173	2.0
5	0.1109	2.5
6	0.0436	1.6
7	0.0272	2.5
8	0.0107	2.3
9	0.0048	

Table 2

Analysis of the convergence of the approximate solution $m_{+h}(z, 1)$ computed by the one-grid method to the true solution $m_+(z, 1)$.

Recall that Theorem 4.1 shows that the one-grid method has accuracy $\mathcal{O}(h)$. Since h is decreased by a factor of two when the parameter m in Table 5.1 is increased by one, we would expect the error to be decreased by a factor two as well. Looking at the last column of Table 5.1 we observe that most of the numbers are sufficiently close to two, in order to conclude that the numerical convergence analysis gives evidence for the theoretical convergence analysis.

For the two-grid method the relevant error corresponding to (4.13) is

$$\mathcal{E}_{m,m^*}^N = \|(m_+)_h^N - (m_+)_h\|_{E_h},$$

where $(m_+)_h^N$ is the approximate solution to the discrete version of (5.10) computed by the two-grid method computed at discretization level $h = 2^{-m}$ with the iteration number N and the coarse grid defined by m^* . To test the convergence rate for the two grid method we have for different choices m^* and

N computed the error \mathcal{E}_{m,m^*}^N . The fine grid parameter is fixed at $m = 10$. As above, we have chosen $k = 1$. Table 5.1 contains the results. As expected

$m^* \setminus N$	0	1	2	3	4	5	6	7
6	0.36	0.049	0.014	0.0036	0.00094	0.00037	8.4e-05	2.9e-05
7	0.21	0.025	0.0071	0.0018	0.00045	0.00018	4.1e-05	1.5e-05
8	0.094	0.011	0.0031	0.00078	0.00019	7.6e-05	1.8e-05	6.5e-06
9	0.03	0.0037	0.0010	0.00026	6.2e-05	2.5e-05	6.9e-06	3.0e-06

Table 3

Error \mathcal{E}_{m,m^*}^N for different choices of N and m^* for the two-grid method. In each case we have chosen the fine grid parameter $m = 10$.

we see immediately from Table 5.1 that the error decreases as the iteration number N grows and as h^* decays (m^* grows). From a more detailed inspection we can draw two conclusions: First, the error ratio $\mathcal{E}_{m,m^*}^{N+1}/\mathcal{E}_{m,m^*}^N$ seems to be independent of m^* (i.e. h^*) and seems to vary with N in a way which is not obvious. Second, the error ratio $\mathcal{E}_{m,m^*}^N/\mathcal{E}_{m,m^*+1}^N$ seems to be independent of N and seems to grow with m^* . The numerical analysis indicates that there is an intimate connection between the discretization level, the iteration number, and the error. However, the results in Table 5.1 do not explicitly support the results given in Theorem 4.2.

6 Conclusion

We have presented a method for computing the solution to $\bar{\partial}$ -equations of the form $\bar{\partial}w = T(k)\overline{w(k)}$. One-grid and two-grid versions of the multigrid method of Vainikko [38,33] are applied with a FFT implementation. We prove that the accuracy of the method is order h . We show that $\bar{\partial}$ -equations in the form above appear naturally in the context of the inverse conductivity problem, which is the underlying mathematical model in electrical impedance tomography (EIT). With the use of the implementations we solved first the forward problem of computing the scattering transform from a known conductivity, and second the inverse problem of computing the conductivity from the scattering transform. Both problems were based on solving a $\bar{\partial}$ -equation, and the results show that we have a fast and reliable implementation of a solver for such equations. Moreover the numerical results give evidence for the accuracy of the methods.

7 Acknowledgments

The work of K.K. was supported by MaPhySto, the Centre for Mathematical Physics and Stochastics, funded by the Danish National Research Foundation. The work of J.M. was supported by the National Science Foundation grant DMS-0104861. The work of S.S. was supported by Grant-in-Aid for JSPS Fellows (No. 00002757) of the Japan Society for the Promotion of Science. The authors thank G. Vainikko for helpful discussions and T. Eirola, M. Huhtanen and J. v. Pflaler for pointing out correct manipulation of real and imaginary parts of the solution when using GMRES.

References

- [1] M. Ablowitz and H. Segur, On the evolution of packets of water waves, *J. Fluid Mech.* **92**, 691 (1979).
- [2] M. Ablowitz, D. Bar Yaacov, and A. S. Fokas, On the inverse scattering transform for the Kadomtsev-Petviashvili equation, *Studies in Appl. Math.* **69**, 135 (1983).
- [3] R. A. Adams, *Sobolev Spaces* (Academic Press, 1975).
- [4] K. Atkinson, *An Introduction to Numerical Analysis* (Wiley, second edition, 1989).
- [5] J. A. Barceló, T. Barceló and A. Ruiz, Stability of the inverse conductivity problem in the plane for less regular conductivities, *J. Differential Equations* **173**, 231, (2001).
- [6] R. Beals and R. R. Coifman, Scattering, transformations spectrales et équations d'évolution non linéaire. I-II, in *Goulaouic-Meyer-Schwartz Seminar, 1981/1982*, Exp. No. XXI, 9. École Polytechnique (1982).
- [7] R. Beals and R. R. Coifman, Multidimensional inverse scattering and nonlinear partial differential equations, *A.M.S.* **43**, 45 (1985).
- [8] R. Beals and R. R. Coifman, The D-bar approach to inverse scattering and nonlinear evolution equations, *Physica* **18**, 242 (1986).
- [9] R. Beals and R. R. Coifman, The spectral problem for the Davey–Stewartson and Ishimori hierarchies, in *Nonlinear evolution equations: Integrability and spectral methods*, p 15–23, Manchester University Press (1988).
- [10] M. Boiti, J–P. Leon, M. Manna, and F. Pempinelli, On a spectral transform of a KdV-like equation related to the Schrödinger operator in the plane, *Inverse Problems* **3**, 25 (1987).

- [11] R. M. Brown and G. Uhlmann, Uniqueness in the inverse conductivity problem for nonsmooth conductivities in two dimensions, *Comm. Partial Differential Equations* **22**, 1009 (1997).
- [12] A. P. Calderón, On an inverse boundary value problem, in *Seminar on Numerical Analysis and its Applications to Continuum Physics*, p 65, Soc. Brasileira de Matemática (1980).
- [13] Y. Chen, A fast, direct algorithm for the Lippmann–Schwinger integral equation in two dimensions, *Adv. Comp. Math.* **16**, 175 (2002).
- [14] M. Cheney, D. Isaacson, and J. C. Newell, Electrical Impedance Tomography, *SIAM Review* **41**, 85 (1999).
- [15] A. Davey and K. Stewartson, On three-dimensional packets of surface waves, *Proc. Royal Soc. London Ser. A* **338**, 101 (1974).
- [16] T. Eirola, M. Huhtanen, and J. von Pfaler Solution methods for \mathbb{R} -linear problems in \mathbb{C}^n , *Helsinki University of Technology Institute of Mathematics Research Reports* **A454** (2002).
- [17] L. D. Faddeev, Increasing solutions of the Schrödinger equation, *Sov. Phys. Dokl.* **10**, 1033 (1966).
- [18] A. S. Fokas and M. J. Ablowitz, The inverse scattering transform for multidimensional 2+1 problems, in *Nonlinear Phenomena*, K.B. Wolf, ed. *Lecture Notes in Physics* (Springer, Berlin, 1984).
- [19] T. Hohage, On the numerical solution of a three-dimensional inverse medium scattering problem, *Inverse Problems* **17**, 1743 (2001).
- [20] K. Knudsen, On the Inverse Conductivity Problem, Ph.D. thesis, Department of Mathematical Sciences, Aalborg University, Denmark (2002).
- [21] K. Knudsen, A new direct method for reconstructing isotropic conductivities in the plane, *Physiol. Meas.* **24**, 391 (2003).
- [22] K. Knudsen and A. Tamasan, Reconstruction of less regular conductivities in the plane, *Aalborg University, Department of Mathematical Sciences Research Reports* R-2003-04 (2003), to appear in *Comm. Partial Differential Equations*
- [23] L. Liu, Stability estimates for the two-dimensional inverse conductivity problem, Ph.D. thesis, Department of Mathematics, University of Rochester, New York (1997).
- [24] J. L. Mueller and S. Siltanen, Direct reconstructions of conductivities from boundary measurements, *SIAM J. Sci. Comput.* **24**, 1232 (2003).
- [25] J. L. Mueller, S. Siltanen, and D. Isaacson, A direct reconstruction algorithm for electrical impedance tomography, *IEEE Trans. Med. Im.*, **21**, 555 (2002).
- [26] A. I. Nachman, Global uniqueness for a two-dimensional inverse boundary value problem, *Ann. of Math.* **143**, 71 (1996).

- [27] A. I. Nachman, Reconstructions from boundary measurements, *Ann. of Math.* **128**, 531 (1988).
- [28] A. Nachman and M. J. Ablowitz, A multi-dimensional inverse scattering method, *Studies in Appl. Math.* **71**, 243 (1984).
- [29] R. G. Novikov, An inversion formula for the attenuated X-ray transform, *Ark. Mat.* **40**, 145 (2002).
- [30] R. G. Novikov, On the range characterization for the two-dimensional attenuated x-ray transformation, *Inverse problems* **18**, 677 (2002).
- [31] R. G. Novikov and G. M. Khenkin, The $\bar{\partial}$ -equation in the multidimensional inverse scattering problem, *Uspekhi Mat. Nauk.*, **42**, 93 (1987).
- [32] Y. Saad and M. H. Schultz, GMRES: a generalized minimal residual algorithm for solving nonsymmetric linear systems, *SIAM J. Sci. Statist. Comput.*, **7**, 856 (1986).
- [33] J. Saranen and G. Vainikko, *Periodic Integral and Pseudodifferential Equations with Numerical Approximation* (Springer, 2002).
- [34] S. Siltanen, J. Mueller, and D. Isaacson, An implementation of the reconstruction algorithm of A. Nachman for the 2-D inverse conductivity problem, *Inverse Problems* **16**, 681 (2000).
- [35] S. Siltanen, J. Mueller, and D. Isaacson, Reconstruction of high contrast 2-D conductivities by the algorithm of A. Nachman, in *Proceedings of the 2000 conference on Radon transforms and tomography*, ed. Quinto et al, 241 (2001).
- [36] T. Tsai, The associated evolution equations of the Schrödinger operator in the plane, *Inverse Problems* **10**, 1419 (1994).
- [37] G. Vainikko *Multidimensional weakly singular integral equations* (Springer Lecture Notes in Mathematics 1549, 1993).
- [38] G. Vainikko, Fast solvers of the Lippmann–Schwinger equation, in *Direct and Inverse Problems of Mathematical Physics* (Newark, DE), Kluwer Acad.; Publ, Dordrecht, Int. Soc. Anal. Appl. Comput. **5**, 423 (2000).
- [39] I. N. Vekua, *Generalized Analytic Functions* (Pergamon Press 1962).
- [40] A. P. Veselov and S. P. Novikov, Finite-gap two-dimensional potential Schrödinger operators, explicit formulas and evolution equations, *Sov. Math. Dokl.* **30**, 588 (1984).

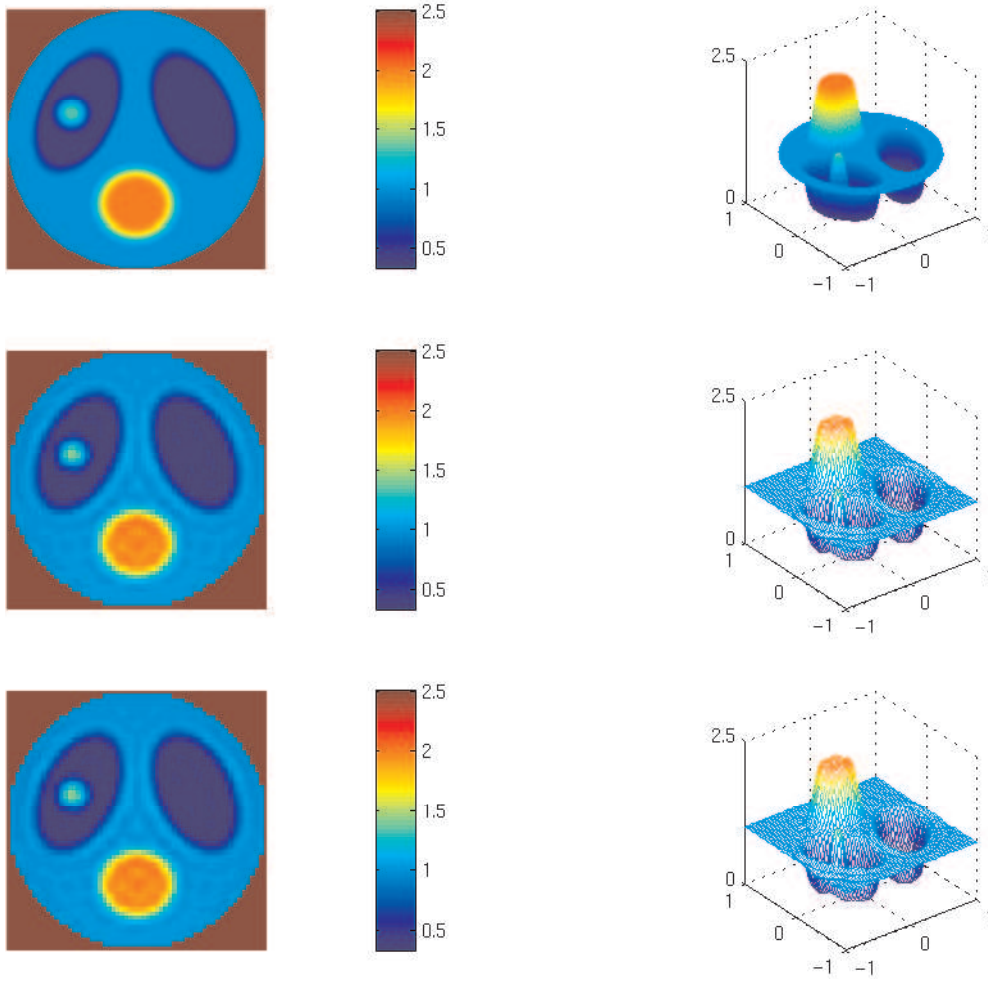


Fig. 3. Top row: original conductivity. Middle row: conductivity γ_1 reconstructed by the one-grid method. Bottom row: conductivity γ_2 reconstructed by the two-grid method.